Preparation and Characterization of Fire Retardant Nano-Filler from Oil Palm Empty Fruit Bunch Fibers

Naheed Saba,[a,*] Paridah Md. Tahir, [a,*] Khalina Abdan,[b] and Nor Azowa Ibrahim [c]

The possibilities of utilizing an abundantly available agricultural waste, oil palm empty fruit bunch (OPEFB) fibers, for the development of nano-filler was investigated. The aim was to develop fire retardant nano-fillers from OPEFB fiber through grinding, chemical treatment (bromine water and $SnCl_2$), and cryogenic crushing, followed by a high energy ball milling process. The structural, morphological, and thermal properties of nano-fillers were investigated by X-ray diffraction (XRD) and transmission electron microscopy (TEM). The analysis revealed that the particle size distribution was reduced from micro to nano size in the range of around 14 to 100 nm. Scanning electron microscopy (SEM) observations revealed that the nanoparticles of OPEFB had irregular shapes. The elemental composition of the OPEFB were investigated by elemental dispersive X-ray analysis (EDX), showing the presence of tin, carbon, oxygen, chlorine, and bromine elements both before and after ball milling. Further, thermo-gravimetric analysis (TGA) and differential scanning calorimetry (DSC) indicated that the developed nanofillers exhibited enhanced thermal properties compared to the untreated fibers. Such results suggest that the developed nano-filler can be used for the fabrication of nanocomposites with improved fire retardancy.

Keywords: Oil palm empty fruit bunch fibers; High energy ball milling; Nano-filler; Structural properties; Morphological properties; Thermal properties

Contact information: a: Laboratory of Biocomposite Technology, Institute of Tropical Forestry and Forest Products (INTROP), Universiti Putra Malaysia, 43400 UPM Serdang, Selangor, Malaysia; b: Department of Biological and Agricultural Engineering, Faculty of Engineering, Universiti Putra Malaysia, 43400 UPM Serdang, Selangor, Malaysia; c: Department of Chemistry, Faculty of Science, Universiti Putra Malaysia, 43400 UPM Serdang, Selangor, Malaysia;
** Corresponding authors: naheedchem@gmail.com; parida.introp@gmail.com*

INTRODUCTION

As science and technology become more advanced, scientists are focusing on eco-environmental experiments to develop niche applications involving naturally available plant fibers, agricultural wastes, and biomass materials. Natural fibers are the most abundant and renewable bio-based resources of nature (Majeed *et al*. 2013). They consist of cellulose, hemicellulose, lignin, and pectin and have a very complicated structure. Plant-based biomass and lignocellulosic materials are currently the most appropriate and inexpensive precursors for the production of nanomaterials or fillers. Activated carbons, cellulose nanofibers, and cellulosic whiskers from various agricultural wastes, such as wood, sawdust, bagasse, coconut shells, rice husk, rubber wood saw dust, oil palm shell, oil palm ash, and coir pith, are being described by the researchers in their studies (Ioannidou and Zabaniotou 2007; Sen and Kumar 2010; Abdul Khalil *et al*. 2011; Jonoobi *et al*. 2011). These materials develop a great deal of interest as a source of nanometer-sized fillers because of their abundant availability, sustainability, and unique features, such as

large surface area to volume ratio, high stiffness, high flexibility, high tensile strength, and improved thermal and electrical properties compared to commercial or traditional fibers (Abe *et al*. 2007; Bondeson and Oksman 2007; Fahmy and Mobarak 2008; Özgür Seydibeyoğlu and Oksman 2008; Roohani *et al*. 2008).

Nanomaterials have at least one dimension in nanometer range and are categorized into three groups: nanoparticles, nanotubes, and nanolayers, depending on the number of dimensions belonging to the nano range (Saba *et al*. 2014). Nanomaterials are attractive owing to their small size, lower agglomeration levels, narrow size distribution, and high dispersion tendency (Paul *et al*. 2007; Marquis *et al*. 2011).

Recently, the synthesis and characterization of these nanostructured materials have received a lot of attention because of their superior mechanical and thermal properties. The different processes implemented for nano preparation use mechanical treatments, chemical treatments, biological treatments, electrospinning methods, and many more (Frenot *et al*. 2007; Henriksson *et al*. 2007; Abe and Yano 2010; Liu *et al*. 2010). These processes includes a variety of sequentially conveyed methods, such as high energy ball milling, ultra-sonication, co-precipitation, plasma arching, electro-deposition, chemical vapor deposition, and sol-gel processing. These different processes result in different types of nanofibrous materials, depending on the starting materials, pretreatment, and disintegration processes.

A "solid state method", specifically high energy ball milling (HEBM), is a novel approach to obtain nanometer-sized materials (Pilloni *et al*. 2010). HEBM has been found to be suitable for a variety of other materials (Abdul Khalil *et al*. 2011) but was originally developed in the 1970's as an industrial process to effectively produce composites and new alloys (Kong *et al*. 2008). The advantage of this technique is its simplicity and suitability as an alternative for the production of amorphous and crystalline nanomaterials, from both a practical and economical point of view (Paul *et al*. 2007). Furthermore, HEBM produces designed nano-sized particles by simple physical isolation without the need of specific temperature even at low sintering temperatures (Yang *et al*. 2015) and pressure. Research studies have already revealed the development of nano banana, nano palm ash, and nano jute particles from HEBM technique (Abdul Khalil *et al*. 2011; Nagendra *et al.* 2014; Padal *et al.* 2014)

As HEBM is based on solid-state reactions, the technique involves atomic diffusion between crushed samples, the steel milling chamber, and steel balls. In the HEBM, the force of the ball impact is remarkably pronounced, thus producing a homogeneous distribution of components in the resulting solids (Tammaro *et al*. 2014). Recently, ball milling techniques have been used for the dispersion of nano-fillers into polymer matrices at room temperature. HEBM can also be used without the use of solvents and for formulating binary polymer/polymer mixtures (Castrillo *et al*. 2007; Zhang *et al*. 2008; Costantino *et al*. 2009). The functioning and concentration of defects in HEBM depends on the materials being milled, the induced milling speed, and their molecular mobility.

Studies indicate that some conventional products (such as natural fiber reinforced polymer composite) do not adequately fulfill safety and fire resistance requirements (Lee *et al*. 2014), especially in the aerospace, automotive, electronics, building-construction, and biotechnology industries. Hence, the awareness about these materials performance and their response during fire allows the incorporation of fire retardant materials in polymeric materials for development of products for different applications. Fire/flame retardants (FRs) are chemical substances that are added to materials both to inhibit or delay the spread of fire after ignition and to stop the polymer combustion process (Laoutid *et al*. 2009). FRs

are classified as additive and reactive fire retardants based on the modes of their incorporation. The FRs are also classified as gaseous and condensed phase retardants on the basis of their mechanisms.

FRs may be halogen-based (such as bromine and chlorine), or halogen-free, including phosphorus, nitrogen, boron, metal oxide-hydroxide minerals (based on aluminum and magnesium), metals (molybdenum, tin), and antimony trioxide. Besides, the traditional FRs, nano-fillers as FRs are appealing to researchers as they can confer an extraordinary level of fire retardation and are quite attractive from both an industrial and academic perspective. They can deliver distinct advantages over traditional FRs during production, as only a small amount of additive may be needed thus (*i.e*., only 2 to 5 wt. % compared to 40 to 70 wt.%) resulting in improved recycling.

The prime objective of this work is the proper utilization of oil palm empty fruit bunch bio-wastes (OPEFB), which is abundant, cheap and easily available, by converting it into fire retardant nano filler. Malaysia alone produces 6.93 million tons of waste OPEFB biomass from oil palm industries, after removing oil from oil palm fruit bunch (OPFB), thus creating a big disposal threat to the environment (Ismail and Shaari 2010). Improper handling of these bio-wastes leads to environmental and health hazards, as it can generate pollution, eutrophication and other disturbances for both terrestrial and aquatic life (Li *et al*. 2011).

This research work focused on the study of structural, morphological, and thermal properties of the developed fire retardant nano-fillers for their suitability in the fabrication of FR nanocomposites for varied applications. This study thus aimed to introduce, create, manipulate, and explore the use of bio-agricultural waste material (OPEFB fibers) in nanotechnology field to beneficial applications in a new way.

EXPERIMENTAL

Materials

The OPEFB fibers were obtained from MPOB, Bangi-Selangor, Malaysia. Bromine water and tin chloride ($SnCl_2$) were procured from NR Medicare Sdn. Bhd., Selangor, Malaysia. The purchased chemicals were used without any further purification. The chemical composition of OPEFB fibers are given in Table 1.

Table 1. Composition (%) of OPEFB Fibers Obtained from MPOB, Malaysia

Component	Composition (%)
Cellulose	43.70
Hemicellulose	29.02
Lignin	13.33
Ash	3.31

Preparation of FR Nano Filler from OPEFB Fiber

The synthesis of nano-filler or particle from naturally available OPEFB fiber involved the following steps in series.

Physical treatment

Raw OPEFB fiber was physically treated by means of dewaxing, followed by washing and drying steps. The OPEFB fibers were dewaxed through soxhlet extraction, using n-hexane as solvent, washed with distilled water to remove extra physical impurities, and finally dried in an air oven for 24 h at 60 ^{o}C. The dried fiber are then processed for grinding in a mechanical grinder, to ground for 60-mesh size.

Chemical treatment

The ground OPEFB fibers were chemically treated, with saturated bromine (3% W/V; with the molecular weight M= 159.82 g/mol) water firstly for 24 h. The fibers were then removed and washed thoroughly with distilled water several times until its pH became neutral (to be free from acid resulting from use of hydrobromic acid, HBr), followed by drying in an air oven at 380 ±5 K, until a constant weight was attained. The brominated OPEFB fibers were treated with stannous chloride solution, followed by boiling, separation, and finally drying in the air oven at 380 ±5 K. During the drying process, the formed OPEFB fiber turned black due to the formation of tin oxide during heating in the atmosphere (Avila and Rodriguez-Paez 2009).

Cryogenic crushing

The black, chemically treated OPEFB fibers were ground to powder with a cryogenizer to further reduce the size under chilled inert nitrogen gas conditions. The cryogenizing involved a combination of severe shearing in the refiner, followed by high-impact crushing under liquid nitrogen (Chakraborty *et al*. 2005).

HEBM processing

Cryogenized OPEFB fibers were converted to a well-defined homogeneous nano-powder through the usage of an 8000D Mixer/Mill HEBM. The HEBM process imparted sufficient energy to break the bundles of OPEFB, obtained from cryogenic crushing, into single nano fibers. The ball mill was loaded with stainless steel balls with a powder weight ratio of 10:1 in the stainless steel chamber. The high energy ball mill was run without any solvent at 1100 rpm (rate per minute). The milled OPEFB were dried in an air oven for 24 h, in order to prevent further agglomeration, and preserved in dry sealed plastics to avoid contact with moisture.

For simplification during the characterization of different stages of the formed OPEFB fibers, the abbreviations shown in Table 2 were used.

Table 2. Nomenclature of OPEFB Fibers, Brominated OPEFB Fibers, and Brominated-$SnCl_2$ Treated OPEFB Fibers

Sample description	Abbreviation
Untreated OPEFB fiber	R-OPEFB
Brominated OPEFB fiber	B-OPEFB
$SnCl_2$+Br_2 treated OPEFB fiber	SB-OPEFB

Characterization

Transmission electron microscopy (TEM)

The morphology and size distribution of particles in the nano-OPEFB fillers/ particles were studied using transmission electron microscopy (TEM; Hitachi-7100,

Japan). For the analysis, the dried sample was dissolved in acetone and dispersed by sonication with ultrasonicator (JP Selecta 3000512, Spain) for 20 min. A drop of the colloidal dispersion containing OPEFB nano particles was transferred onto a carbon coated 300-mesh copper grid and allowed to dry completely at room temperature before being examined by TEM.

X-ray diffraction (XRD)

Powdered X-ray diffraction (XRD) analyses were carried out in order to understand the crystallinity of the nano-OPEFB particles. The patterns were collected by using X'Pert, an X-ray diffractometer (Siemens XRD D5000, USA), and Ni-filtered Cu Kα radiation at an angular incidence of 0° to 80° (2θ angle range).

Scanning electron microscopy (SEM)

The microstructure and morphological characteristics of the nano-particles/filler were studied using scanning electron microscopy (SEM) after gold coating by EMITECH, K575X (Korea) peltier cooled, followed by micrographs with NOVA NANO SEM 230 (USA) field emission instrument.

Elemental dispersive X- ray analysis (EDX)

The EDX analyses were conducted to obtain the elemental composition of the samples using the NOVA NANO SEM 230 (USA) instrument.

Fourier transform infrared spectroscopy (FTIR)

The Fourier transform infrared spectroscopy (FTIR) analyses were performed (Shimadzu 81001; Japan) to investigate the changes in surface functional groups of the R-OPEFB (untreated), B-OPEFB, SB-OPEFB fibers in the range of 4000 to 400 cm^{-1}.

Thermogravimetric analysis (TGA)

The thermal stability of OPEFB samples were characterized using a thermogravimetric analyzer (TGA Q500 TA Instruments, USA). TGA of R-OPEFB, B-OPEFB, SB-OPEFB fiber and nano filler were carried out at a heating rate of 20 °C/min under a nitrogen atmosphere from 30 to 800 °C range.

Differential scanning calorimetry (DSC)

The differential scanning calorimetry (DSC) studies were carried out using a DSC Q20 TA instrument (USA) with aluminum sample pan in an argon atmosphere with a heating rate of 5°C/min and a static argon flow of 50 mL/min. Specimens of approximately 10 mg were scanned over a temperature range of 25 to 200 °C.

RESULTS AND DISCUSSION

Transmission Electron Microscopy (TEM)

Figures 1a and b show the TEM image of the nano-OPEFB sample along with its size distribution. The particles appeared spherical, uniform, and mono-dispersed with an average size distribution of 6 nm. This result is quite similar to that obtained in the case of oil palm ash and nano banana fibers on treatment with HEBM (Nagendra *et al*. 2014).

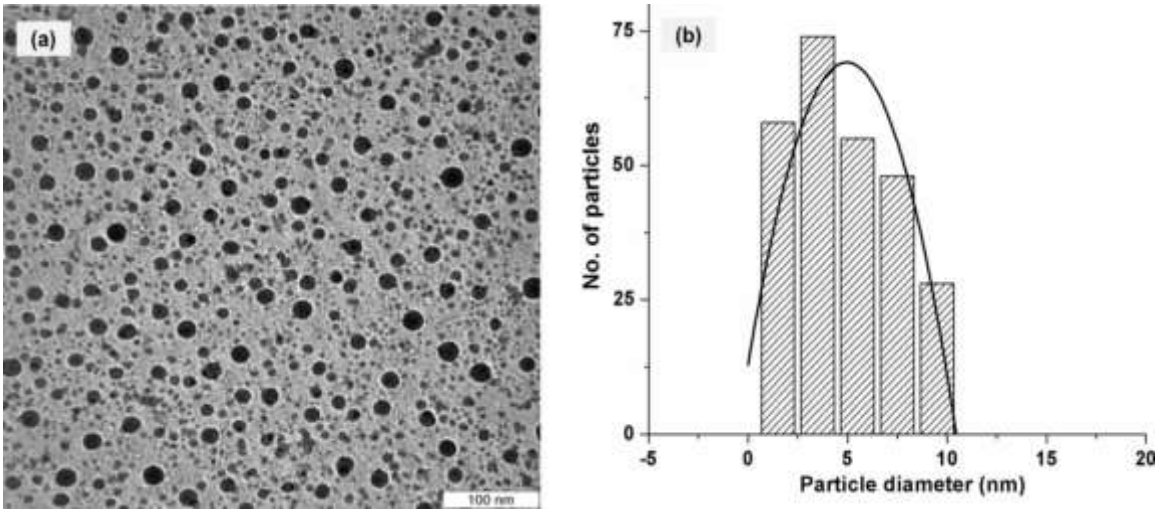

Fig. 1. TEM image of the nano-OPEFB **filler** (a) along with its particle size distribution (b)

X-Ray Diffraction (XRD)

Figure 2 shows the comparison of the XRD patterns of raw and nano-OPEFB filler, *i.e*., samples taken before and after being subjected to HEBM. The pattern shows two broad, high intense peaks around 18° and 25° in the raw OPEFB sample, which sharpen after HEBM treatment. This suggests the persistence of the same material even after the ball milling process. Also, a small peak for OPEFB fiber before ball milling, observed around 35°, disappeared after the ball milling.

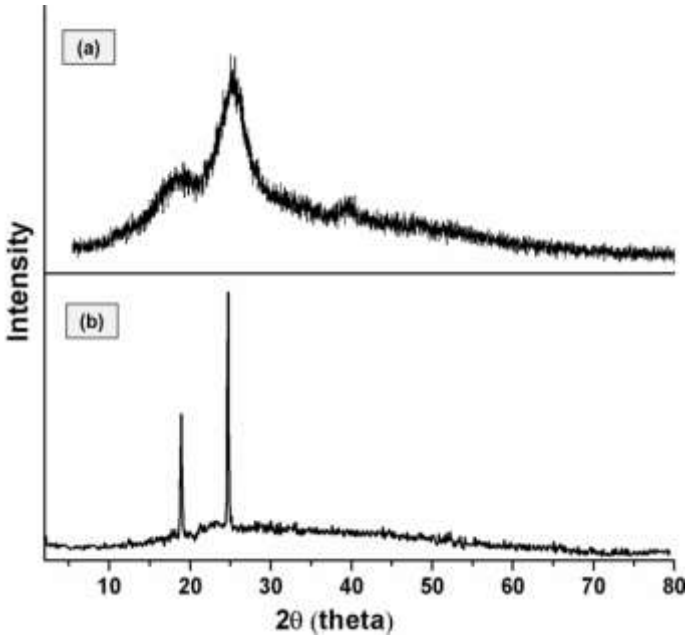

Fig. 2. Comparison of the XRD patterns of raw and OPEFB filler before (a) and after (b) HEBM

From the XRD figure, it is evident that nano-OPEFB possessed a smaller crystallinity index, as indicated by two pointed peaks, in comparison to R-OPEFB (untreated), having one broad peak and two small peaks in the diffractogram. The decrease in crystallinity indicated that the mechanically operated HEBM induced a significant

decrease in the particle size from the raw material to the nano-OPEFB filler. Also, a saturation stage for size reduction was observed only after 8 h of ball milling when subjected to a rate of 1100 rpm. These results are similar to coir, jute, and banana nanofibers, where the crystalline size of the nanofibers were reduced with an increase in milling time and the size reduction became constant after completion of the optimum milling time (Sen and Kumar 2010; Nagendra *et al*. 2014; Padal *et al*. 2014). Another interesting XRD study made on nano-class F-fly ash revealed that HEBM of 60 h, significantly decreased the crystallinity and, in turn, increased the amorphous domains as compared to the starting raw materials (Paul *et al*. 2007).

Scanning Electron Microscopy/EDX

The SEM micrograph of OPEFB samples before and after the HEBM treatment was carried out to assess surface morphology at micron and submicron levels. The corresponding images are shown in Fig. 3a and b. Figure 3a shows that the SEM of R-OPEFB has an irregularly shaped porous sponge-like structure.

Figure 3b shows that after the HEBM process, the OPEFB fibers were crushed to fine nano particles. The nano-OPEFB showed some smaller particles with the same irregular shape. The irregular shape of the nano-fillers decreases the required filler loading to meet strength objectives and enhances the fracture strength of the polymeric-composites (Abdul Khalil *et al.* 2011). These results are in agreement with other results, as in the cases of nano-ash from oil palm (Abdul Khalil *et al*. 2011), nano fly ash (Paul *et al*. 2007), and nano coir fiber (Sen and Kumar 2010).

The presence of such irregularly shaped structures is especially useful for FR applications because of the non-uniform transmittance of heat at each point in time. The developed nano-OPEFB FR materials will effectively delay the spread of fire and flammable gases during exposure to heat and fire.

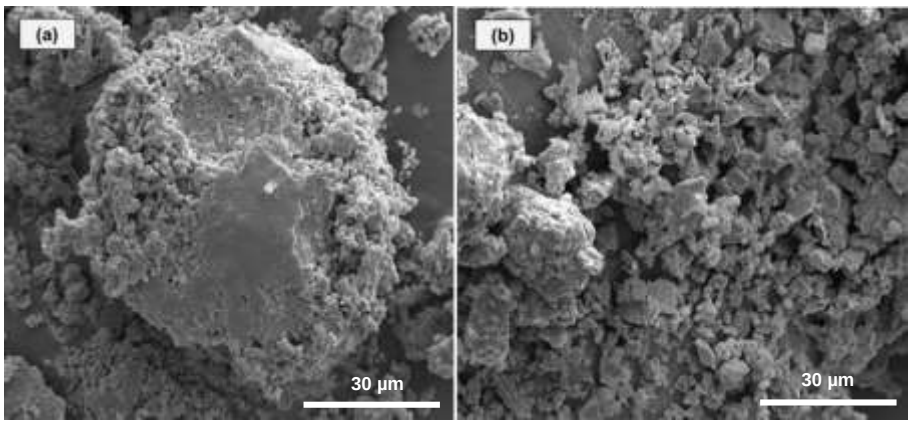

Fig. 3. Comparison of the micrographs of OPEFB fibers before (a) and after (b) HEBM

The elemental composition of the OPEFB samples (before and after the HEBM process) recorded through the SEM equipped EDX analyzer are shown in Fig. 4. The appearance of EDX peaks in the graphs corresponding to Cl, Sn, Br, O, and C confirm the presence and persistence of those elements in both the samples. Further, the EDX spectra provide evidence for the occurrence of a bromination reaction on the surface of OPEFB fiber, as indicated by the presence of bromine related peaks in both of the samples. However, the appearance of very small peaks for bromine in comparison to the sharp peaks

of chlorine may be due to the dominating electronegative role played by chlorine element in the presence of high energy X-ray beams. Moreover, the peak can only be obtained after repeated filtration by the use of an X-ray filter, which further improves the detection sensitivity.

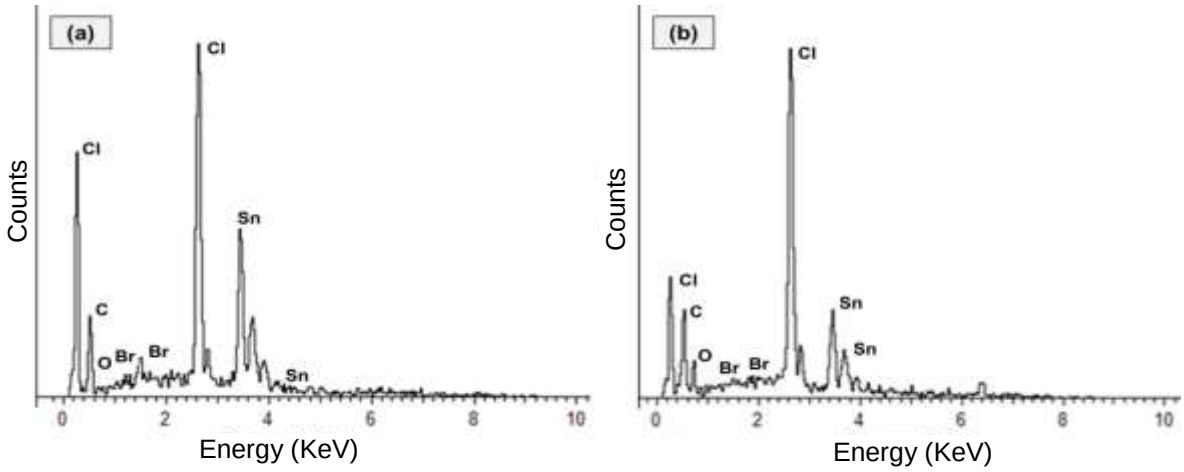

Fig. 4. Comparison of the EDX spectrums of OPEFB samples before (a) and after (b) the ball milling process

Fourier Transform Infrared Spectroscopy (FTIR)

In general, the plant fibers are made of three components: cellulose, hemicellulose and lignin. These components are primarily composed of alkanes, esters, aromatics, ketones, and alcohols with different oxygen containing functional groups. Hence, the FTIR analyses were performed on the (R-, B-, SB-) OPEFB fibers in order to fully understand the nature of the functional groups.

Figure 5 shows the FTIR spectra of R-OPEFB, B-OPEFB, and SB-OPEFB fibers. An absorption band around 3350-3400 cm^{-1} and 3900 cm^{-1} in all of the spectra corresponds to the stretching vibrations of –OH and C-H, respectively. Similarly, the presence of peaks around 1750 cm^{-1} and 1480 cm^{-1} for all the samples corresponds to C=O stretching and C-C aromatic skeletal vibrations for the lignin groups, respectively. The peak around 1260 cm^{-1} (from C-O-C stretching) and 1150 cm^{-1} are generated from the ether linkage due to the groups of hemicellulose (Fahma *et al*. 2010; Rosa *et al*. 2012; Mohamad Haafiz *et al*. 2013). The appearance of these peaks in all the samples indicates persistent traces of hemicellulose without any disturbance to its structure, even after chemical treatment with bromine water and $SnCl_2$ media, which is similar to nano-fibrils from *Helicteres isora* (Chirayil *et al*. 2014).

For the two samples B-OPEFB and SB-OPEFB, the appearance of a sharp, bright peak around 580 cm^{-1} corresponds to the stretching vibrations of C-Br bonds. Also, the constricted bond around 780 cm^{-1} in the SB-OPEFB fiber shows the vibrations due to metal halogen bonds (Meng *et al*. 2009; Sen and Kumar 2010). From the analysis of all the FTIR spectra, it can be confirmed that the SB-OPEFB material containing the elements Sn, Cl, and Br adsorbed onto the surface of the fibers, while still maintaining the basic structural components of cellulose, hemicellulose, and lignin.

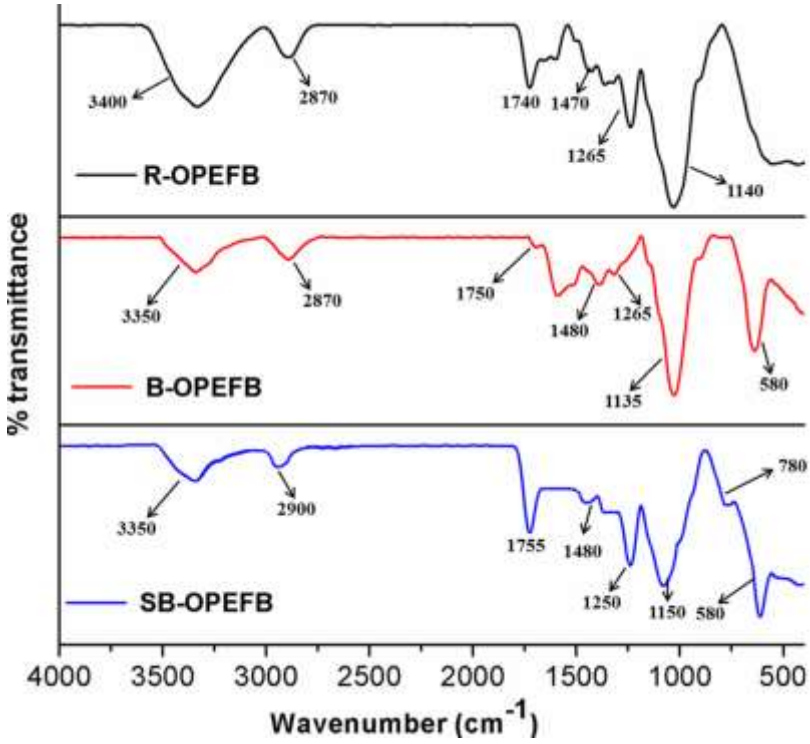

Fig. 5. Comparison of the FTIR spectrum of untreated R-OPEFB and B-OPEFB against SB-OPEFB fibers

Thermal Properties

TGA results for R-OPEFB, B-OPEFB, SB-OPEFB, and nano-particles/filler are shown in Fig. 6. All the samples (R-OPEFB, B-OPEFB, SB-OPEFB fibers) showed an initial mass change from room temperature to 200 °C. This corresponds to an endothermic loss of moisture in the sample, which was also observed in the DSC curve. In the case of the R-OPEFB fibers, the degradation started above 250 °C; whereas in the other samples, degradation started below 250 °C. These results indicate that the bromination decreased the thermal stability of the OPEFB fibers. The degradation of all material was sharp up to 380 °C. However, above 380 °C, the weight change was gradual. In the case of R-OPEFB material, one observes that a similarly steep change in weight loss occurred from 280 °C to 380 °C. A similar trend in thermal behavior also has been reported for coir fibers and jute fibers (Sen and Kumar 2010; Padal *et al*. 2014).

Above 380 °C, the degradation of R-OPEFB fiber was faster compared to the others. The weight of material left at higher temperatures was less for R-OPEFB compared to other samples of OPEFB fibers, which decomposed completely at 700 °C. The char obtained was significantly greater for SB-OPEFB fibers in comparison to B-OPEFB (14.17%) and R-OPEFB fibers (10.85%). This is favorable for fire retardancy.

The TGA of nano-OPEFB shows three degradation stages. The first degradation stage started before 200 °C and the second stage started around 250 to 360 °C, which was similar to the case of SB-OPEFB fibers. After the second stage, the percentage weight loss is only 22% (at 360 °C) for the nano-OPEFB and 26% for the SB-OPEFB fiber. The third degradation stage was observed near 506 °C, with a further weight loss of only 7%. This small weight loss indicates the stability of the material at various stages. Finally, the residual char obtained was close to 29% for nano-OPEFB, which is considerably greater than that obtained in the case of untreated (R-OPEFB, 10%) and B-OPEFB fibers (14%).

This increased formation of residual char after exposure to the very high temperature of 700 °C is attributed to the presence of complex structures that result from the bromine and tin elements. The persistence of these elements does not allow the heat to pass through easily. The analysis of these results confirms that the nano-OPEFB can serve as a potential inhibitor when used for FR applications.

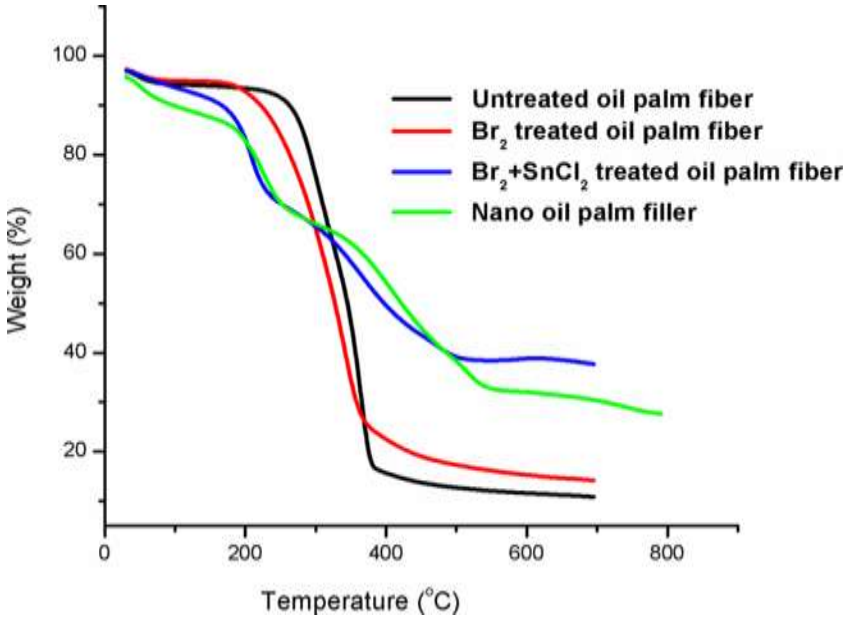

Fig. 6. TGA comparison of the graphs of R-OPEFB, B-OPEFB, SB-OPEFB, and nano-OPEFB fillers

The DSC curves of R-OPEFB, B-OPEFB, SB-OPEFB, and nano-OPEFB filler are shown in Fig. 7. The curves for R-OPEFB and B-OPEFB fibers show one small and one broad endothermic peak near 140 °C and 180 °C, respectively. The observation of endothermic peaks is attributed to the loss of adsorbed moisture (the same was reported from TGA graph). As the temperature was increased from 180 °C to higher temperature, the graph for both R- and B-OPEFB fibers showed exothermic behavior without any further peak formation. The exothermic peaks are due to the degradation of the OPEFB fibers.

Furthermore, the DSC of B-OPEFB fiber near 200 °C shows the peak to be less exothermic in nature as compared to the R-OPEFB fiber. The heat change for B-OPEFB fiber was small when compared to the raw fiber in all cases, which is similar to the results obtained for coir fiber (Sen and Kumar 2010).

The thermal behavior of nano- and SB-OPEFB fibers was altogether different from what was observed from the R-OPEFB and B-OPEFB fibers. The broad endothermic peak near 100 °C for SB-OPEFB and the two peaks near 45 °C and 140 °C for nano-OPEFB are due to the loss of the same moisture content from the fibers. Further, the SB-OPEFB graph shows only one characteristically small exothermic peak near 120 °C and above 140 °C. Correspondingly for nano-OPEFB filler, the significant point is that, at temperatures above 160 °C, the curve shows an exothermic transition similar to SB-OPEFB, in contrast to other two samples. But at higher temperature it shows shifting towards an endothermic transition. Moreover, at considerably higher temperatures above 180 °C, the DSC graphs of both the nano- and SB-OPEFB fibers showed some endothermic transitions without any peak indications, which was the same result as has been observed with DSC of coir fiber (Sen

and Kumar 2010). This indicates the release of a low amount of heat during the degradation. The property of heat evolution at higher temperatures is relatively favorable for fire-retardant related applications. The DSC perfectly revealed that as the temperature increased from 180 °C, both R- and B-OPEFB fiber showed exothermic behavior. However, nano and SB-OPEFB showed endothermic nature, which is favorable for FRs materials. These results indicate that the nano OPEFB filler has considerably higher thermal stability as compared to the raw OPEFB fibers.

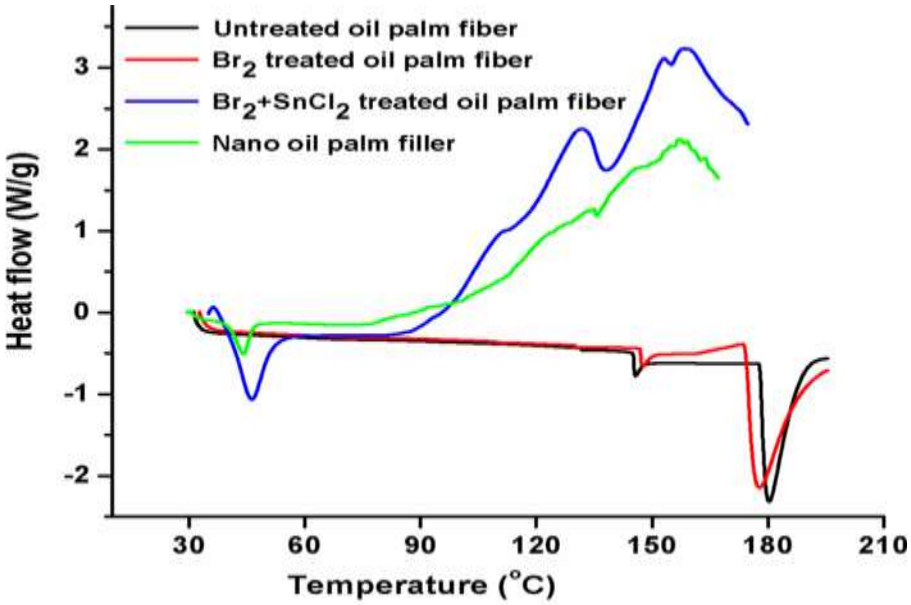

Fig. 7. Comparison of the DSC of R-OPEFB, B-OPEFB, SB-OPEFB, and nano-OPEFB fillers

CONCLUSIONS

1. High energy ball milling proved to be a sophisticated technique for the reduction of macromolecular to nano-sized fine particles, supporting their excellent versatility, scalability, and cost effectiveness.
2. The FTIR spectra and EDX analysis clearly showed that bromination and $SnCl_2$ treatment lead to adsorption of the elements Br, Sn, and Cl onto the surface of the fiber as indicated by the observation of corresponding peaks in the spectra/graphs.
3. Developed nano-particles possessed improved thermal stability, as explored by TGA and DSC results.
4. The surface morphologies shown by SEM, TEM, and XRD further illustrate the irregular amorphous shape of the nano-OPEFB material.
5. This research supports the assertion that the resulting nano-structural additive materials developed from agricultural OPEFB wastes can be incorporated as fire retardant nano-fillers in different polymer matrices to fabricate nano-composites for distinctive industrial applications.

ACKNOWLEDGMENTS

The first author thanks Universiti Putra Malaysia for providing International Graduate Research Fellowship (IGRF). The authors would also like to acknowledge the Universiti Putra Malaysia for supporting this research through Putra Grant No. 9420700.

REFERENCES CITED

Abdul Khalil, H. P. S., Fizree, H. M., Jawaid, M., and Alattas, O. S. (2011). "Preparation and characterization of nano structured materials from oil palm ash – A bioagricultural waste from oil palm mill," *BioResources* 6(4), 4537-4546. DOI: 10.15376/biores.6.4.4537-4546

Abe, K., Iwamoto, S., Yano, H. (2007). "Obtaining cellulose nanofibers with a uniform width of 15 nm from wood," *Biomacromolecules* 8, 3276-3278. DOI: 10.1021/bm700624p

Abe, K., and Yano, H. (2010). "Comparison of the characteristics of cellulose microfibril aggregates isolated from fiber and parenchyma cells of moso bamboo (*Phyllostachys pubescens*)," *Cellulose* 17, 271-277. DOI:10.1007/s10570-009-9382-1

Avila, H. A., and Rodríguez-Páez, J. E. (2009). "Solvents effects in the synthesis process of tin oxide," *J. Non Cryst. Solids* 355, 885-890.

Bondeson, D., and Oksman, K. (2007). "Polylactic acid/cellulose whisker nanocomposites modified by polyvinyl alcohol," *Compos. Part A Appl. Sci. Manuf.* 38, 2486-2492. DOI:10.1016/j.compositesa.2007.08.001

Castrillo, P. D., Olmos, D., Amador, D. R., and González-Benito, J. (2007). "Real dispersion of isolated fumed silica nanoparticles in highly filled PMMA prepared by high energy ball milling," *J. Colloid Interface Sci.* 308, 318-324. DOI:10.1016/j.jcis.2007.01.022

Chakraborty, A., Sain, M., and Kortschot, M. (2005). "Cellulose microfibrils: A novel method of preparation using high shear refining and cryocrushing," *Holzforschung* 59, 102-107. DOI:10.1515/HF.2005.016

Chirayil, C. J., Joy, J., Mathew, L., Mozetic, M., Koetz, J., and Thomas, S. (2014). "Isolation and characterization of cellulose nanofibrils from *Helicteres isora* plant," *Ind. Crops Prod*. 59, 27-34. DOI:10.1016/j.indcrop.2014.04.020

Costantino, U., Bugatti, V., Gorrasi, G., Montanari, F., Nocchetti, M., Tammaro, L., and Vittoria, V. (2009). "New polymeric composites based on poly(ε-caprolactone) and layered double hydroxides containing antimicrobial species," *ACS Appl. Mater. Interfaces* 1, 668-677. DOI:10.1021/am8001988

Fahma, F., Iwamoto, S., Hori, N., Iwata, T., and Takemura, A. (2010). "Isolation, preparation, and characterization of nanofibers from oil palm empty-fruit-bunch (OPEFB)," *Cellulose* 17, 977-985.

Fahmy, T. Y. A., and Mobarak, F. (2008). "Nanocomposites from natural cellulose fibers filled with kaolin in presence of sucrose," *Carbohydr. Polym*. 72, 751-755. DOI:10.1016/j.carbpol.2008.01.008

Frenot, A., Henriksson, M. W., and Walkenström, P. (2007). "Electrospinning of cellulose-based nanofibers," *J. Appl. Polym. Sci*. 103, 1473-1482. DOI:10.1002/app.24912

Ioannidou, O., and Zabaniotou, A. (2007). "Agricultural residues as precursors for activated carbon production - A review," *Renew. Sustain. Energy Rev.* DOI:10.1016/j.rser.2006.03.013

Ismail, H., and Shaari, S. M. (2010). "Curing characteristics, tensile properties and morphology of palm ash/halloysite nanotubes/ethylene-propylene-diene monomer (EPDM) hybrid composites," *Polym. Test.* 29, 872-878. doi:10.1016/j.polymertesting.2010.04.005

Jonoobi, M., Khazaeian, A., Tahir, P. M., Azry, S. S., and Oksman, K. (2011). "Characteristics of cellulose nanofibers isolated from rubberwood and empty fruit bunches of oil palm using chemo-mechanical process," *Cellulose* 18, 1085-1095. DOI:10.1007/s10570-011-9546-7

Kong, L. B., Zhang, T. S., Ma, J., and Boey, F. (2008). "Progress in synthesis of ferroelectric ceramic materials via high-energy mechanochemical technique," *Prog. Mater. Sci.* 53, 207-322. DOI:10.1016/j.pmatsci.2007.05.001

Laoutid, F., Bonnaud, L., Alexandre, M., Lopez-Cuesta, J. M., and Dubois, P. (2009). "New prospects in flame retardant polymer materials: From fundamentals to nanocomposites," *Mater. Sci. Eng. R Reports* 63, 100-125. DOI:10.1016/j.mser.2008.09.002

Lee, C. H., Mohd Sapuan Salit, and Hassan, M. R. (2014). "A review of the flammability factors of kenaf and allied fibre reinforced polymer composites," *Adv. Mater. Sci. Eng*. 514036, 1–8.

Li, Y., Ding, X., Guo, Y., Rong, C., Wang, L., Qu, Y., Ma, X., and Wang, Z. (2011). "A new method of comprehensive utilization of rice husk," *J. Hazard. Mater*. 186, 2151-2156. DOI:10.1016/j.jhazmat.2011.01.013

Liu, H., Liu, D., Yao, F., and Wu, Q. (2010). "Fabrication and properties of transparent polymethylmethacrylate/cellulose nanocrystals composites," *Bioresour. Technol*. 101, 5685-5692. DOI:10.1016/j.biortech.2010.02.045

Majeed, K., Jawaid, M., Hassan, A., Abu Bakar, A., Abdul Khalil, H. P. S., Salema, A. A, and Inuwa, I. (2013). "Potential materials for food packaging from nanoclay/natural fibres filled hybrid composites," *Mater. Des.* 46, 391-410. DOI:10.1016/j.matdes.2012.10.044

Meng, T., Gao, X., Zhang, J., Yuan, J., Zhang, Y., and He, J. (2009). "Graft copolymers prepared by atom transfer radical polymerization (ATRP) from cellulose," *Polymer (Guildf).* 50, 447-454. DOI:10.1016/j.polymer.2008.11.011

Mohamad Haafiz, M. K., Eichhorn, S. J., Hassan, A., and Jawaid, M. (2013). "Isolation and characterization of microcrystalline cellulose from oil palm biomass residue," *Carbohydr. Polym.* 93, 628-634. DOIi:10.1016/j.carbpol.2013.01.035

Nagendra, P. S., Prasad, V. V. S., and Ramji, K. (2014). "Synthesis of bio-degradable banana nanofibers," *Int. J. Innov. Technol. Res*. 2, 730-734.

Padal, K. T. B., Ramji, K., and Prasad, V. V. S. (2014). "Isolation and characterization of jute nano fibres," *IJMERR* 3, 422-428.

Paul, K. T., Satpathy, S. K., Manna, I., Chakraborty, K. K., and Nando, G. B. (2007). "Preparation and characterization of nano structured materials from fly ash: A waste from thermal power stations, by high energy ball milling," *Nanoscale Res. Lett.* 2, 397-404. DOI:10.1007/s11671-007-9074-4

Pilloni, M., Nicolas, J., Marsaud, V., Bouchemal, K., Frongia, F., Scano, A., Ennas, G., and Dubernet, C. (2010). "PEGylation and preliminary biocompatibility evaluation of

magnetite-silica nanocomposites obtained by high energy ball milling," *Int. J. Pharm*. 401, 103-112. DOI:10.1016/j.ijpharm.2010.09.010

Roohani, M., Habibi, Y., Belgacem, N. M., Ebrahim, G., Karimi, A. N., and Dufresne, A. (2008). "Cellulose whiskers reinforced polyvinyl alcohol copolymers nanocomposites," *Eur. Polym. J*. 44, 2489-2498. DOI:10.1016/j.eurpolymj.2008.05.024

Rosa, S. M. L., Rehman, N., De Miranda, M. I. G., Nachtigall, S. M. B., and Bica, C. l. D. (2012). "Chlorine-free extraction of cellulose from rice husk and whisker isolation," *Carbohydr. Polym.* 87, 1131-1138.

Saba, N., Tahir, P., and Jawaid, M. (2014). "A review on potentiality of nano filler/natural fiber filled polymer hybrid composites," *Polymers (Basel)* 6, 2247-2273. DOI:10.3390/polym6082247

Sen, A. K., and Kumar, S. (2010). "Coir-fiber-based fire retardant nano filler for epoxy composites," *J. Therm. Anal. Calorim*. 101, 265-271.

Tammaro, L., Vittoria, V., and Bugatti, V. (2014). "Dispersion of modified layered double hydroxides in poly(ethylene terephthalate) by high energy ball milling for food packaging applications," *Eur. Polym. J.* 52, 172-180. DOI:10.1016/j.eurpolymj.2014.01.001

Yang, H. K., Lee, J. H., Hong, W. T., Jang, H., Moon, B. K., Jeong, J. H., and Je, J. Y. (2015). "Preparation and photoluminescence properties of nano-sized $SrZnO_2$:Sm_3þ phosphor powders obtained by high-energy ball milling," *Ceram. Int*. 41, 991-994.

Zhang, G., Schlarb, A.K., Tria, S., Elkedim, O. (2008). Tensile and tribological behaviors of PEEK/nano-SiO_2 composites compounded using a ball milling technique," *Compos. Sci. Technol*. 68, 3073-3080. DOI:10.1016/j.compscitech.2008.06.027

Article submitted: March 13, 2015; Peer review completed: May 22, 2015; Revised version received and accepted: May 28, 2015; Published: June 3, 2015.
DOI: 10.15376/biores.10.3.4530-4543